# A Hepta-band WWAN/LTE Antenna Design for Metal-rimmed Smartphone Applications

**Yun-Fei Qiang and Yong-Ling Ban**
Institute of Electromagnetics
University of Electronic Science and Technology of China
2006 Xi-Yuan Avenue, Western High-Tech District, Chengdu, Sichuan 611731, China

**Abstract**— A simple direct-fed dual-loop antenna capable of providing hepta-band WWAN/L TE operation under surroundings of an unbroken metal rim in smartphone applications is proposed. The greatest highlight of this proposed antenna is that it provides a simple and effective solution for an unbroken metal-rimmed smartphone. The unbroken metal rim with 5 mm in height embraces the system circuit board of $130 \times 70\,\mathrm{mm}^2$. Two no-ground portions of $10 \times 70\,\mathrm{mm}^2$ and $5 \times 70\,\mathrm{mm}^2$ are set on the top and bottom edge of the system circuit board, respectively. In-between the two separate no-ground portions, there is a system ground of $115 \times 70\,\mathrm{mm}^2$ connected with the unbroken metal rim by a small grounded patch. This proposed dual-loop antenna is capable of covering GSM850/900/DCS/PCS/UMTS2100/LTE2300/2500 operating bands. Detailed design considerations of the proposed antenna are described and both experimental and simulation results are also presented and discussed.

## 1. INTRODUCTION

In recent years, smartphones have entered into a rapid development period and have gradually become the main communication tools. Furthermore, a smartphone with an unbroken metal rim has become an obvious trend. The metal rim can not only provide sufficient mechanical strength to extend the service life of the smartphone, but also can possess a wonderful appearance, which is very desirable for consumers.

Recently, several promising solutions have been demonstrated which can resolve the effects of the metal rim [1, 2]. For example, reported in [1], it has shown a method to reduce the effects of the metal rim by inserting three gaps and two grounded patches. By judiciously choosing the locations of the gaps and the grounded patches, this method can alleviate the effects of the metal rim. However, the radiation efficiency will be dramatically reduced if these gaps are directly touched by fingers or hands. By adding several grounded patches between the bottom system ground and the unbroken metal rim, a compact slot antenna is proposed in [2]. The two slots are fed by the same feeding strip, which can cover five WWAN bands of GSM850/900/DCS/PCS/UMTS2100 operation. Seen from the above discussion, none of them can provide enough bandwidth to cover WWAN/LTE operating bands.

To alleviate this problem, a simple direct-fed dual-loop antenna capable of providing hepta-band WWAN/LTE operation under surroundings of an unbroken metal rim in smartphone applications is proposed. The unbroken metal rim, which is directly fed by a 50-$\Omega$ mini coaxial feed line, is connected to the system ground by a small grounded patch. The biggest merit of the proposed antenna is that it keeps the integrity of the metal rim and provides sufficient bandwidth to cover hepta-band WWAN/LTE operation, which makes it very promising for metal-rimmed smartphone applications.

Compared with some other promising antennas [3–5] whose bandwidth is widened by utilizing matching network requiring additional board area and cause insertion loss, the proposed simple dual-loop antenna structure without any matching network not only can simplify the difficulty of antenna tuning in the final optimization process, but also can guarantee its low fabrication cost and high radiation efficiency.

## 2. PROPOSED ANTENNA CONFIGURATION

Figure 1(a) shows the geometry of the proposed dual-loop antenna formed by an unbroken metal rim for WWAN/LTE smartphones, whose detailed structure and optimized dimensions are given in Fig. 1(b). As illustrated in Fig. 1(a), a 0.8-mm thick FR4 substrate of relative permittivity 4.4 and loss tangent 0.024 is used as the system circuit board. The system circuit board of $130 \times 70\,\mathrm{mm}^2$ is embraced by an unbroken metal rim whose height is of 5 mm and thickness is of 0.3 mm. The distance between the system circuit board and the metal rim is 2 mm [2]. Two no-ground portions of $10 \times 70\,\mathrm{mm}^2$ and $5 \times 70\,\mathrm{mm}^2$ are set on the top and bottom edge of the system circuit board, respectively. In-between the two separate no-ground portions, there is a system ground plane with the length of 115 mm and the width of 70 mm.

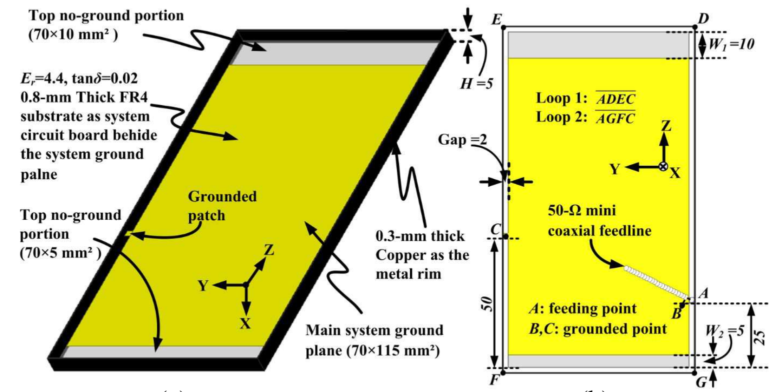


(a) (b)

Figure 1: Proposed antenna configuration: (a) Geometry of the metal-rimmed antenna for hepta-band operations in smartphone applications; (b) Detailed dimensions of the proposed antenna (Unit: mm).

Seen from the Fig. 1(b), a 50-Ω mini coaxial feed line is employed to excite the antenna connected to the feeding point (point A) and the grounded point (point B). The distance between the feeding point and the bottom edge of the system circuit board is 25 mm. The unbroken metal rim is divided into two loops by a small grounded patch which has a distance of 50 mm away from the bottom edge of the system circuit board.

## 3. RESONANT MODES AND CURRENT DISTRIBUTION

To fully comprehend the excited modes of the proposed dual-loop antenna, two reference antennas (Ref-1 and Ref-2) are introduced. Fig. 2(a) shows the simulated input reactance of the proposed antenna and the reference antennas, the case with Loop 1 only (Ref-1) and the case with Loop 2 only (Ref-2). The modes generated by the Ref-1 (Loop 1 only) and the Ref-2 (Loop 2 only) are marked as $M_{0.5n\lambda,\,L_1}$ and $M_{0.5n\lambda,\,L_2}$, respectively, where $n$ represents the $n$-th order modes. Seen from the Fig. 2, the proposed dual-loop has five resonant modes ($M_{0.5\lambda,\,L_1}$, $M_{0.5\lambda,\,L_2}$, $M_{1\lambda,\,L_2}$, $M_{2\lambda,\,L_1}$, $M_{1.5\lambda,\,L_2}$ or $M_{2.5\lambda,\,L_1}$). Seen from Fig. 2(a), two modes of Ref-1 $M_{1\lambda,\,L_1}$, $M_{1.5\lambda,\,L_1}$ are not appeared in the proposed antenna. This is explained as follows: the resonant frequency of the $M_{1\lambda,\,L_1}$ is very closed to the resonant frequency of the $M_{0.5\lambda,\,L_2}$. Around the resonant frequency of the $M_{1\lambda,\,L_1}$, the inductive reactance of the $M_{1\lambda,\,L_1}$ is compensated by the larger capacitive reactance of the $M_{0.5\lambda,\,L_2}$. Finally, in the proposed antenna, only one resonant mode is appeared in the proposed antenna. The above theory can also be used to explain the behavior of the $M_{1.5\lambda,\,L_1}$. Fig. 2(b) shows the corresponding simulated return loss of the Fig. 2(a). The multi-resonant character for

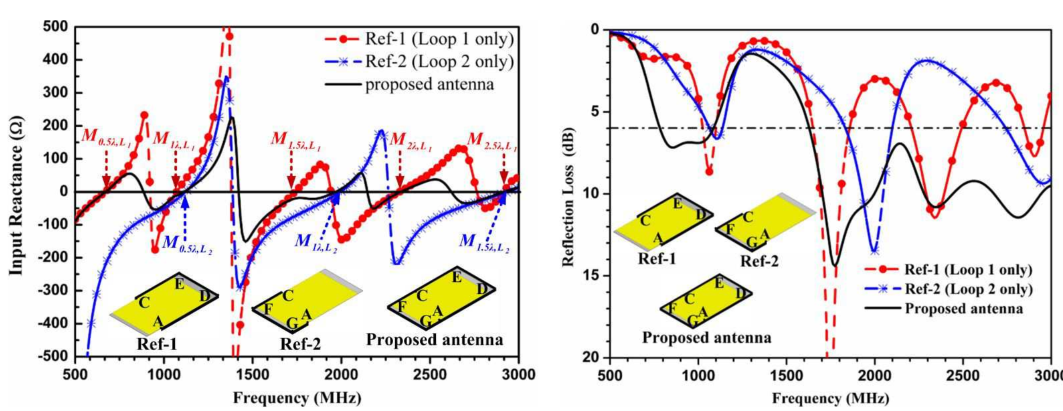


(a) (b)

Figure 2: (a) Simulated input reactance and (b) simulated return loss, respectively, of the proposed antenna and the case with Loop 1 only (Ref-1), and the case with Loop 2 only (Ref-2).

both Ref-1 and Ref-2 can be easily seen from Fig. 2(b). The bandwidth for each resonant mode of Ref-1 and Ref-2 is very narrow. However, by employing the multi-resonant modes provided by the Ref-1 and Ref-2, the proposed antenna can provide two wide operating bands of 824–960 MHz and 1710–2690 MHz, respectively.

In order to distinguish these resonant modes, simulated surface vector current distributions of the proposed antenna at frequencies of 0.67 GHz, 1.13 GHz, 1.98 GHz, 2.35 GHz and 2.93 GHz, which corresponds to the modes of $M_{0.5\lambda,L_1}$, $M_{0.5\lambda,L_2}$, $M_{1\lambda,L_2}$, $M_{2\lambda,L_1}$, $M_{1.5\lambda,L_2}$ (or $M_{2.5\lambda,L_1}$), are plotted in Figs. 3(a), (b), (c), (d) and (e), respectively. It can be clearly seen that the simulated surface current has a null point along the Loop 1 at 0.67 GHz. This indicates that the proposed antenna operates in the $M_{0.5\lambda,L_1}$ which is the fundamental mode of the Loop 1. The other modes of $M_{0.5\lambda,L_2}, M_{1\lambda,L_2}, M_{2\lambda,L_1}$ can be analyzed easily from Fig. 2 and the surface current distributions of the corresponding resonant frequencies in Figs. 3(b), (c), (d).

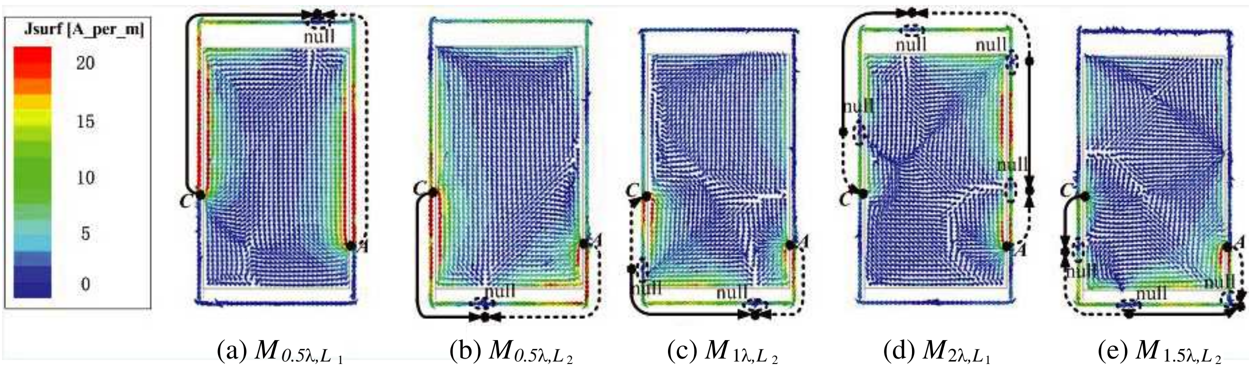


Figure 3: Simulated surface current distributions in the proposed antenna at the corresponding resonant frequencies of (a) 0.67 GHz; (b) 1.13 GHz; (c) 1.98 GHz; (d) 2.35 GHz; (e) 2.93 GHz.

## 4. RESULTS AND DISCUSSION

The simulated results are gained by Ansoft HFSS version 13, while the measured results are tested by using an Agilent N5247A vector network analyzer. Fig. 4 presents the measured and simulated return losses for the prototype, which are in with good agreement.

The measured total efficiency and antenna gain of the fabricated antenna are presented in Fig. 5. For the lower band of GSM850/900 (824–960 MHz), the antenna gain varies from about 1.2 to 2.0 dBi and the total efficiency is about 62–79%, which are acceptable for practical application. For the desired upper bands of DCS/PCS/UMTS2100/LTE2300/2500 (1710–2690 MHz), the obtained antenna gain is 1.0–3.9 dBi and the corresponding total efficiency is larger than 54%. As a result, the measured radiation characteristics of the proposed antenna within the operating band are suitable for meeting the requirement for smartphone systems [6, 7].

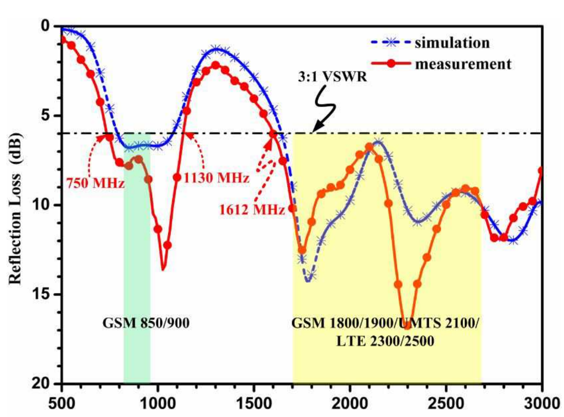


Figure 4: Measured and simulated $S$ parameters.

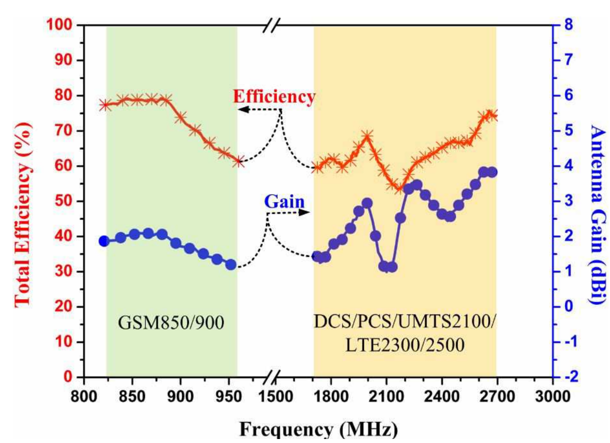


Figure 5: Measured radiation efficiency.

## 5. CONCLUSION

A simple direct-fed dual-loop antenna capable of providing hepta-band WWAN/LTE operation under surroundings of an unbroken metal rim in smartphone applications is proposed and studied in this paper. The obtained measured results including return loss and total efficiency are presented, which can meet the requirements for smartphone systems. The greatest highlight is that the proposed antenna can keep the integrity of the metal rim, which is very novel for metal-rimmed smartphone applications.

## REFERENCES

1. Guo, Q. X., R. Mittra, F. Lei, and Z. R. Li, "Interaction between internal antenna and external antenna of mobile phone and hand effect," *IEEE Trans. Antennas Propag.*, Vol. 61, No. 2, 862–870, 2013.
2. Yuan, B., Y. Cao, G. F. Wang, and B. Cui, "Slot antenna for metal-rimmed mobile handsets," *IEEE Antennas Wirel. Propag. Lett.*, Vol. 11, 1334–1337, 2012.
3. Valkonen, R., M. Kaltiokallio, and C. Icheln, "Capacitive coupling element antennas for multi-standard mobile handsets," *IEEE Trans. Antennas Propag.*, Vol. 61, No. 5, 2783–2791, 2013.
4. Zheng, M., H. Y. Wang, and Y. Hao, "Internal hexa-band folded monopole/dipole/loop antenna with four resonances for mobile device," *IEEE Trans. Antennas Propag.*, Vol. 60, No. 6, 2880–2885, 2012.
5. Ban, Y. L., Y. F. Qiang, Z. Chen, K. Kang, and J. L. W. Li, "Low-Profile narrow-frame antenna for seven-band WWAN/LTE smartphone applications," *IEEE Antennas Wirel. Propag. Lett.*, Vol. 13, 463–466, 2014.
6. Ban, Y. L., J. H. Chen, S. Yang, J. Li, and Y. Wu, "Low-profile printed octaband LTE/WWAN mobile phone antenna using embedded parallel resonant structure," *IEEE Trans. Antennas Propag.*, Vol. 61, No. 7, 3889–3894, 2013.
7. Ban, Y. L., C. L. Liu, and L. W. Li, "Small-size coupled-fed antenna with two printed distributed inductors for seven-band WWAN/LTE mobile handset," *IEEE Trans. Antennas Propag.*, Vol. 61, No. 11, 5780–5784, 2013.